A comparison of L1 and L2 norms as temporal constraints for reconstruction of undersampled dynamic contrast enhanced cardiac scans with respiratory motion

G. Adluru[1,2], and E. V. DiBella[2]

[1]Electrical & Computer Engineering, University of Utah, Salt Lake City, Utah, United States, [2]Radiology, University of Utah, Salt Lake City, Utah, United States

Introduction: Dynamic contrast enhanced (DCE) MRI is used to track the uptake and washout patterns of the injected contrast agent into a region of interest. Cardiac DCE is used to find regions of reduced blood flow to the myocardium. The recently proposed constrained reconstruction framework [1-3] can be used to accelerate the data acquisition. The method can be used to obtain better coverage, temporal and spatial resolution as compared to standard acquisitions. The temporal constraint term plays a significant role in determining the quality of reconstructions obtained for cardiac DCE data [3]. The constrained reconstruction methods in [2, 3] used an L2 norm in the temporal constraint for reconstructing images from undersampled data. The method [2] was able to achieve an acceleration factor of five when there was minimal or no respiratory motion in the data. In the presence of motion, the method using the L2 norm [2] was not fully able to resolve the artifacts. In [3] an L1 norm spatial constraint was used along with an L2 norm in the temporal constraint. It is well known that in image denoising using an L1 norm in the spatial constraint better preserves the spatial edges as compared to using an L2 norm [4]. Here we compare the use of an L1 norm in the temporal constraint to the use of an L2 norm in image reconstruction. The reconstruction methods are compared and evaluated on both simulated and actual undersampled cardiac radial data.

Methods: Constrained reconstruction of undersampled data is performed by iteratively minimizing a cost function which consists of a data fidelity term and constraint terms [1-3]. The data fidelity term minimizes the mismatch between the estimated solution and the acquired data. The constraints are based on the general properties of the estimated solution. Two such cost functions C_1 and C_2 are shown in equation (1) and equation (2) respectively. The first term in the equations is the data fidelity term in which W is the undersampling matrix with ones where the data are sampled and zeros where the data are missing, F represents the Fourier transform, $\tilde{m}$ is the reconstructed image estimate, $\|.\|_2$ is the L2 norm and $\tilde{d}$ is the acquired undersampled k-space data. The second term in the equations is the temporal constraint term which is based on the temporal characteristics of the data. The temporal constraint in equation (1) uses an L2 norm of the temporal gradient, while the temporal constraint in equation (2) corresponds to an L1 norm ($\|.\|_1$) of the temporal gradient. α_1 is the weighting factor for the temporal constraint and ε in equation (2) is a small positive constant. For a given temporal gradient, the temporal constraint in C_1 has higher a penalty as compared to that in C_2. This means that in a perfusion dataset which has respiratory motion, the constraint in C_2 would better allow for sudden changes in time dimension as compared to that in C_1. Also from a compressed sensing point of view [5-7], using an L1 norm as a constraint exploits the implicit sparsity in the temporal gradient of the data. The third term in the equations is the spatial constraint term with an L1 norm of the spatial gradient [4] and α_2 is the corresponding weighting factor. The spatial constraint helps in further reduction of the artifacts while preserving the spatial edges in the images.

$$C_1 = \left\|WF\bar{m} - \bar{d}\right\|_2^2 + \alpha_1 \left\|\nabla_t \bar{m}\right\|_2^2 + \alpha_2 \left\|\sqrt{\nabla_x \bar{m}^2 + \nabla_y \bar{m}^2 + \varepsilon}\right\|_1 \quad (1)$$

$$C_2 = \left\|WF\bar{m} - \bar{d}\right\|_2^2 + \alpha_1 \left\|\sqrt{\nabla_t \bar{m}^2 + \varepsilon}\right\|_1 + \alpha_2 \left\|\sqrt{\nabla_x \bar{m}^2 + \nabla_y \bar{m}^2 + \varepsilon}\right\|_1 \quad (2)$$

Reconstructions using equations (1) and (2) were tested on data with simulated undersampling and actual undersampled radial data. Simulated undersampled data was obtained from fully sampled Cartesian k-space data. Cartesian k-space data was acquired from a Siemens 3T Trio scanner and the data was undersampled offline using approximate radial lines on a Cartesian grid. Actual undersampled radial perfusion data was acquired from a Siemens 3T Trio scanner using a modified turboFLASH sequence [8] which used a saturation pulse every fifth slice and obtained each slice in ~60-70 msec.

α_1 in C_1 and C_2 was chosen by using the L-curve method as in [2] without using the spatial constraint. α_2 was then chosen empirically (by fixing α_1) to minimize the error in the reconstruction as compared to full data reconstruction in a simulated undersampled dataset and was fixed for other datasets.

Results: Fig 1 compares the reconstructions of a perfusion dataset with minimal respiratory motion for the simulated undersampling case. The reconstructions in Fig 1b and Fig 1c are comparable and match closely with Fig 1a as shown by the absolute difference images in Fig 1d and Fig 1e. Fig 2 compares the results of a different perfusion dataset with significant respiratory motion using simulated undersampled data. In this case Fig 2c is sharper especially around the myocardium and matches better with Fig 2a as compared to Fig 2b. The absolute difference image in Fig 2e has less structure in it as compared to that in Fig 2d. Also the total absolute difference between Fig 2a and Fig 2b is 431 and that between Fig 2a and Fig 2c is 381, which quantifies the relative improvement. Fig 3 compares the reconstructions of the actual undersampled radial data (R~4) with motion. Fig 3a and Fig 3b show the reconstructions obtained by minimizing C_1 and C_2 respectively. Fig 3b has better contrast between the myocardium and the blood pool and is less blurry around the myocardium and papillary muscles as compared to Fig 3a. The zoomed images in Fig 3c and Fig 3d illustrate the point.

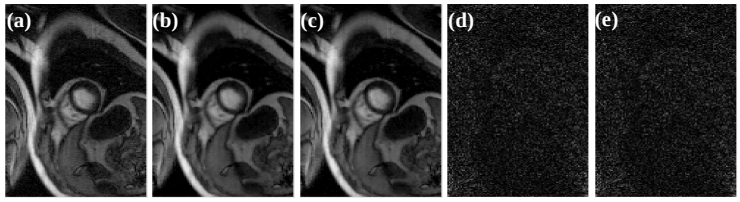

Figure 1. Comparison of reconstructions using simulated undersampled data without respiratory motion. **(a)** Image reconstructed from full data using Inverse Fourier Transform (IFT) at a single time point. **(b)** Corresponding image reconstructed from 25% of full k-space data by minimizing C_1. **(c)** Corresponding image reconstructed from 25% of the data by minimizing C_2. **(d)** Absolute difference image between Fig 1a and Fig 1b. **(e)** Absolute difference image between Fig 1a and Fig 1c.

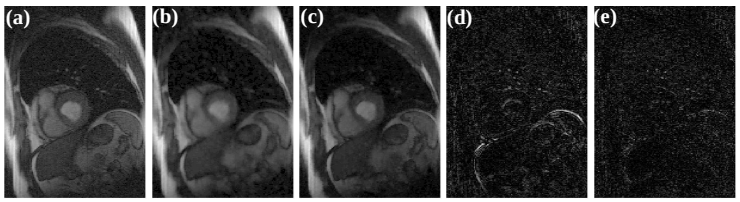

Figure 2. Comparison of reconstructions using simulated undersampled data with respiratory motion. **(a)** Image reconstructed from full data using IFT at a single time point. **(b)** Corresponding image reconstructed from 25% of full k-space data by minimizing C_1. **(c)** Corresponding image reconstructed from 25% of the data by minimizing C_2. **(d)** Absolute difference image between Fig 2a and Fig 2b. **(e)** Absolute difference image between Fig 2a and Fig 2c.

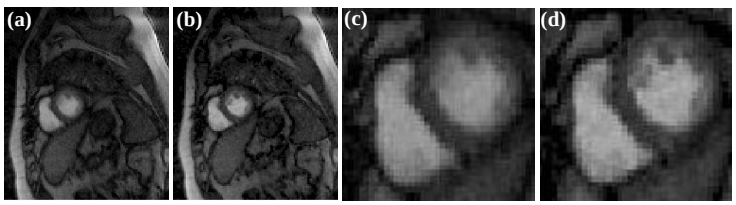

Figure 3. Comparison of reconstructions using actual undersampled radial data with respiratory motion. **(a)** Image reconstructed from R~4 radial data by minimizing C_1. **(b)** Corresponding image reconstructed by minimizing C_2. **(c)** Zoomed image of Fig 3a. **(d)** Zoomed image of Fig 3b.

Conclusion: Using an L1 norm in the temporal constraint helps in obtaining better reconstructions as compared to using an L2 norm especially when the original data has respiratory motion. This is because an L1 norm constraint as in C_2 does not penalize sudden changes as much as the L2 norm constraint as in C_1. The constrained reconstruction method with an L1 norm in the temporal constraint can be used to accelerate cardiac DCE imaging without significant loss in spatial and temporal characteristics.

References: [1] Portniaguine O et al, Proc. ISMRM, 481, 2003. [2] Adluru G et al, MRM, 57:1027-1036, 2007. [3] Adluru G et al, Proc. IEEE ISBI, 109-112, 2007. [4] Rudin LI et al, Physica D, 60:259-268, 1992. [5] Candes EJ et al, IEEE Trans Info Theory, 52:489-509, 2006. [6] Block KT et al, MRM, 57:1086-1098, 2007. [7] Lustig M et al, Proc. ISMRM, 685, 2005. [8] Adluru G et al, Submitted to SCMR 2008.